UDC 546.831:621.039.532.6

HYDROGEN IN ZIRCONIUM
Part 1

T.P. Chernyayeva, A.V. Ostapov
"Nuclear Fuel Cycle" Science and Technology Establishment NSC KIPT, Kharkov, Ukraine
E-mail: chernyaeva@kipt.kharkov.ua; phone: +38(057)335-60-26

The data on hydrogen behavior in zirconium have been systematized. The proposed study deals with a number of basic physicochemical characteristics of the two participants in the Zr–H (H and Zr) reaction, as well as the basic data on Zr–H system in whole. The data on hydrogen atoms position in Zr lattice (predominantly tetragonal voids) and its dynamics are provided. It should be noted that whether the zirconium-dissolved hydrogen has a state of neutral atoms H^0 or ions (H^+, H^-, $H^{\delta-}$, $H^{\delta+}$) is a disputable question, while it is clearly stated that hydrogen is not found in zirconium in the molecular state and does not form bubbles filled with molecular hydrogen gas. The basic principles of interaction of hydrogen with metal (M) are reported. The study presents thermodynamics of hydrogen adsorption and absorption by zirconium. Great attention is paid to the correlation characteristics of M–H system interaction with M position in the periodic table, and evaluating implementation of these correlations with respect to the Zr–H system. The data on the diffusion mobility of hydrogen in zirconium are provided. The collected data are aimed at creating a source data base on interaction in Zr–H system required for investigations on delayed hydride cracking.

INTRODUCTION

More than a semicentennial experience of water-cooled reactors operation demonstrated, sometimes painfully, that hydrogen, accumulated in zirconium structural components (ZSC) in operation, upon reaching a critical density (total or local) is one of the main limiting state criteria of these components [1], [2]. The danger is also aggravated by the fact that the presence of hydrogen in zirconium structural components (ZSC) accumulated during operation, may adversely impact the fuel assembly zirconium components during the subsequent operations of spent nuclear fuel (SNF) handling and long-term storage [3].

The main hydrogen-degradation effects in ZSC during operation are: hydrogen embrittlement (sharp ductility decrease during hydriding), formation of large, massive hydrides (corona defects, blisters) (Fig.1) and delayed hydride cracking (gradual stepped crack growth, induced by simultaneous stress and hydrogen effects) (Fig. 2). Each of these phenomena is based on physicochemical interaction of hydrogen with zirconium: physical adsorption, chemisorption, hydrogen dissolution and diffusion, hydride formation, etc. [4]. That is why, development of a delayed hydride cracking (DHC) concept being the matter of our investigation, must be preceded and supported by the data on chemicophysical interaction of hydrogen with zirconium. Some of the information search results that are being carried out in this direction are presented here.

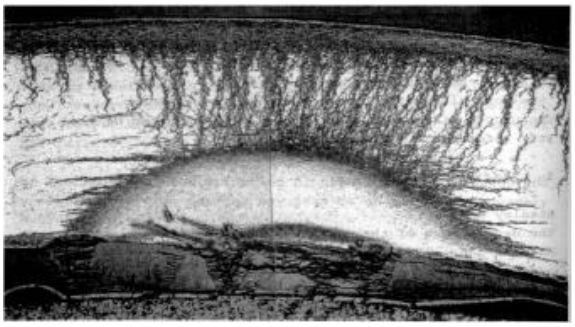

Fig. 1. Massive hydride in fuel rod cladding (corona defect) [5]

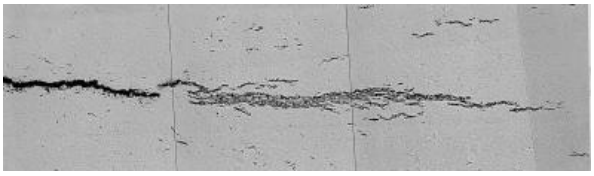

Fig. 2. «Split effect» – fuel rod cladding splitting, induced by destruction with collaboration of hydrogen [6],[7]

In the present investigation, the issues related to hydride crystallography and the properties of zirconium hydrides are discussed only insofar as it is required to develop a basic understanding of the hydrogen/zirconium interaction. We proceeded from the paper size restriction, and the fact that fundamental reviews on the structure and properties of binary hydrides (including zirconium hydrides) were earlier made by Puls [8], Andriyevskiy and Umanskiy [9], [10].

1 HYDROGEN

1.1 Atomic Hydrogen

Hydrogen is the simplest in structure, the smallest and lightest of atoms containing one proton and a single electron. Paradoxically, but this simplicity of electronic structure brings about the unique consequences in respect to chemical and physical properties of the element (its atoms, cations and anions) [11]. In its tendency to a completely vacant or completely filled shell, hydrogen, generally, exhibits three oxidation states: +1, 0, -1, corresponding to electron configurations $1s^0$, $1s^1$ and $1s^2$, respectively. A number of transformations of atomic hydrogen H^0 (protium) into hydride-ion H^{+1} are associated with a fractional change in a number of electrons around the nucleus. During such transformations, the particle size changes considerably. The radius of atomic hydrogen H^0 is 0.10 nm [12]. Attachment of an electron to a hydrogen atom results in a considerable increase in its size: a hydride-ion H^{-1} radius in a free state equals 0.208 nm [12], [13]. However the most notable change in size occurs during the ionization of hydrogen atoms (H^0-$e^-\rightarrow H^{+1}$), which leads to a smaller radius of $0.84184\cdot10^{-6}$ nm [14]. Such difference in size between an atom and its cation (5 orders) is unique. Next 1s element - lithium changes its radius only from 0.155 nm for Li^0 to 0.068 nm for Li^{+1}.

Atomic radius of hydrogen in the molecular H_2 (covalent bond) equals 0.037 nm [11].

Despite its apparent completeness, atomic hydrogen (H^0) is an unstable condition. Being in contact with other atoms or molecules, it will certainly react to form a covalent, proton (cation H^{+1}) or anion (H^{-1}) bond.

Big values of the first ionization energy I = 1312 kJ/mole (13.60 eV) and electron affinity AE= 72.8 kJ/mole (0.75 eV) evidence of a significant difference between the chemical properties of H^{+1} and H^{-1} (Fig. 3) [11]. The binding force of electron with H^n decreases considerably in the order: $H^{+1} > H^0 > H^{-1}$. The result demonstrates the exciting dual physical and chemical properties of hydrogen - it is a strong cation for nonmetals, and a weak anion for metals.

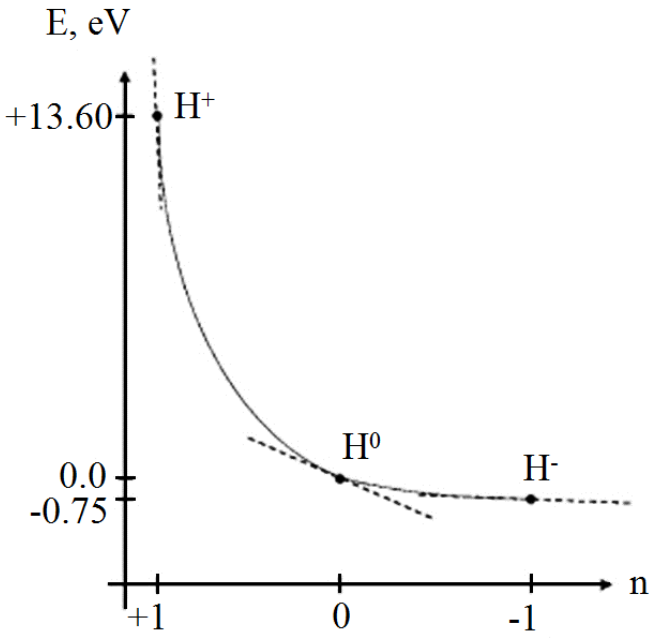

Fig. 3. Hydrogen energy H^n versus oxidation state n. Dotted lines – a derivative of the electron binding force with H^n by electron density. The electron binding force decreases significantly in the order $H^{+1} > H^0 > H^{-1}$[11]

The H–H bonding enthalpy in H_2 is 436 kJ/moleH_2 or 4.52 eV, which is quite close to a strongly bonded oxygen molecule (498.4 kJ/mole or 5.17 eV).

H^{+1} and/or H^{-1} atomic charge changes in accordance with the following reactions [11]:

$$H^{-1}\rightarrow H^0+e^- (\Delta H= +0.75 \text{ eV}); \quad (1)$$

$$H^{+1}+e^-\rightarrow H^0 (\Delta H= -13.60 \text{ eV}); \quad (2)$$

$$2H^0\rightarrow H_2 (\Delta H= -4.52 \text{ eV}); \quad (3)$$

$$H^{-1}+H^{+1}\rightarrow H_2 (\Delta H= -17.37 \text{ eV}). \quad (4)$$

A specific position in the periodic table implies a very significant energy difference between the two states: H^{+1} and H^{-1} (E_p+E_A= 1384.8 kJ/mole (14.35 eV)), resulting in a wide variety of its bonds and phenomena with participation of hydrogen, and certain tendencies in interactions of the element under study with hydrogen, depending on its position in the periodic table [11].

The basic data about atomic hydrogen, which determine the character and intensity of its interaction in contact with other elements, are provided in Table 1.

Table 1

Basic Data on Atomic Hydrogen

Symbol	H [4], [15]
Atomic Number	1 [15]
Electron Configuration	$1s^1$ [15]
Atomic Weight	1.007825 [15]
Absolute Weight	$1.67261 \cdot 10^{-27}$ kg [16]
Nuclear Spin (h/2π)	½ [4], [15]
Nuclear Magnetic Moment	+2.79284 μN [4], [15]
Oxidation State	H^+; H^0; H^-[11]
First Ionization Potential	I = 13.598433 eV [15]
Electron Affinity	EA = 0.75420375 eV [17], [18]
Electronegativeness (Pauling scale)	2.2 [19]; 2.1 [20], [21]
Covalent Radius in H_2	0.037 nm [11]
Orbital Bohr Radius	0.0529 nm [4], [12]
Atomic Hydrogen Radius (protium), H^0	0.120 nm [22]; 0.1 nm [12]
Proton Radius, H^+	$0.84184 \cdot 10^{-6}$ nm [14]
Negative Ion Radius (Protide), H^-	0.208 nm [12], [13]
Thermal Neutron Absorption Section	$0.322 \cdot 10^{-24}$ cm^2 [12]

The size of hydrogen atoms and ions in solid solution and compounds depends on their surroundings (Table 2).

Table 2

Hydrogen Atoms and Ions Size in Solid Solution and Compounds

Hydrogen Sate	Radius of Atoms and Ions
Atomic State of Zr	0.046 nm [23], [24]
Covalent Radius	0.028…0.037 nm depending on surroundings [20]
Effective Ionic Radius H^+	0.018…0.038 nm depending on surrounding anions [4], [25]
Effective Ionic Radius H^-	0.154 nm [20] *

*Note. Effective Ionic Radius H^- depends on the surroundings: Radius H^- in MgH_2 equals 0.13 nm; Radius H^- in $NaBH_4$ equals 0.20 nm [12]. The table provides the most frequent value of anion H for metals.

Since hydrogen is the lightest of atoms, it has the best quantum properties of all other elements (H^0– simple harmonic oscillator) [26], [27].

As already stated, hydrogen atoms cannot bear loneliness; the normal state of hydrogen is H_2(g).

1.2 Molecular Hydrogen H_2

Hydrogen molecule H_2 – is a classic example of a covalent bond that is based on the exchange forces [28]. Under normal conditions, molecular hydrogen is a combination of the two isomers: *ortho*- and parahydrogen [29]. Nuclear magnetic moments (spins) of orthohydrogen (*o*-H_2) have a similar orientation, while those of parahydrogen (p-H_2) have an opposite orientation. Normal hydrogen gas contains ~ 75 % of *o*-H_2 and ~ 25 % of *p*-H_2 [29]. Conversion of *o*-H_2 into *p*-H_2 is accompanied with heat production (~ 1400 kJ/mole), which, however, does not occur without catalysts.

The main properties of molecular hydrogen are presented in Table 3.

Table 3

Main Properties of Molecular Hydrogen

Molar mass	2.01594 [30]
Absolute mass	$3.497 \cdot 10^{-27}$ kg [16]
Ionization potential	I = 15.426 eV [31]
Electron affinity	EA = -0.7 eV [29]
Bond length	0.07416 nm [4]
Bond energy	-4.748 eV [4],[30]
Dissociation energy	4.748 eV [4], [30]
Vibration energy	0.5160 eV [4], [30]
Rotation energy	0.00732 eV [4], [30]
Density in gaseous state	0.0899 kg/m^3[12]
Density of liquid hydrogen	70.811 kg/m^3[12]

High value of the ionization potential I and negative value of electron affinity EA characterize H_2 as a weak electron-donor-acceptor [29], [31], [32]. Electron detachment naturally weakens the H–H bond (Table 5), but electron transfer to the antibinding σ*- MO is much more effective in doing so, decreasing the bond dissociation energy H–H (E_D) (Table 4) [29].

Table 4

Characteristics Of Bonding Forces in Molecule H_2 And Its Ionization States [29]

Molecules and Ions	E_D, kJ/mole	l_{H-H}, nm
H_2	436	0.074
H_2^+	259	0.107
H_2^-	231	0.086

A number of molecular hydrogen properties of are worth special consideration [16]:

- very small size (H–H distance is only 0.074 nm);
- strong influence of nuclear magnetic moments (spins) forming the two isomers: ortho- and parahydrogen, with general symmetric and antisymmetric nuclear spins, respectively;
- low electron density;
- ability to dissociate into atoms.

1.3 Standard Thermodynamic Properties of Hydrogen

For prediction of possibility and completeness of chemical reactions, as well as for state diagram calculations it is necessary to know the initial values of thermodynamic functions and constants for these calculations. The most frequently required data are: standard enthalpy of formation $\Delta_f H^0$ (298.15), standard entropies S^0 (298.15) and standard heat capacities C_p^o (298.15).

Table 5 lists the standard thermodynamic properties of hydrogen (properties of H, H^-, H^+, H_2 at the temperature of 298.15 K and pressure of 0.1 MPa) [33].

Table 5

Standard Thermodynamic Properties of Hydrogen [33]

State	Parameter				
	C_p^o(298.15), J/mole K	S^0(298.15), J/mole K	H^0(298.15), kJ/mole	$\Delta_f H^0$(298.15), kJ/mole	$\Delta_f G^0$(298.15), kJ/mole
H	20.786	114.716	6.197	217.999	203.278
H_2	28.836	130.68	8.467	0	0
H^+	20.786	108.946	6.197	1536.246	1516.990
H^-	20.786	108.960	6.197	139.032	132.282

2 ZIRCONIUM

The basic information about zirconium, which determines its interaction with hydrogen, is provided in Table 6.

Table 6

Some Characteristics of Zirconium

Parameter	Value
1	2
Atomic Weight	A = 91.224 [15]
Atomic number	Z = 40 [15]
Group	IV
Subgroup	IVB – American designation; IVA – European designation
Electron Configuration	[Kr] $4d^2$ $5s^2$ [15]
Ionization Energy: 1st Ionization Potential	6.63390 eV [15]
Spin	5/3 [15]
Magnetic Moment	-1.303 μN [15]
Electron Affinity	EA=0.427±0.014 eV [18], [34]
Electronegativeness (Pauling Scale)	1.33 [35]; 1.4 [36]
Electronegativeness (Allred Rochow Scale)	1.22 [37]
Atomic Radius	R=0.160 nm [38]
Ionic Radius	$r(Zr^{+1})$ = 0.114 nm; $r(Zr^{+2})$ = (0.087±0.007) nm; $r(Zr^{+3})$ = (0.079±0.005) nm; $r(Zr^{+4})$ = (0.072±0.007) nm [39]
Molar Volume	$14.02 \cdot 10^{-6}$ m^3/mole [38]
α⇔β- Transition Temperature	$T_{\alpha/\beta}$= (1135±10) K [33]

Cont. Table 6

1	2
Transition Enthalpy	$\Delta H_{tr\alpha\rightarrow\beta}$ = (4.017±0.3) kJ/mole [33]
Mass Density	$\rho_m = 6.506 \cdot 10^3$ kg/m^3 [33]
Bulk Modulus	B = 97.1 GPa [40]
Melting Temperature	T_m = (2125±15) K [33]
Enthalpy of Melting	ΔH_m = 20.92 kJ /mole [33]
α-Zr Crystal Structure	FCC; a = 0.3232 nm; c = 0.5147 nm [41]
β-Zr Crystal Structure	BCC; a = 0.3609 nm at 862 °C [42]
Cohesive Energy	6.25 eV [42]
Thermal Neutron Absorption Cross-Section	$0.185 \cdot 10^{-24}$ cm^2 [43]

Standard thermodynamic properties of zirconium are presented in Table 7.

Table 7

Standard Thermodynamic Properties of Zirconium [33]

Material	Parameter				
	C_P^0(298.15) J/mole K	S^0(298.15), J/mole K	H^0(298.15), kJ/mole	$\Delta_f H^0$(298.15), kJ/mole	$\Delta_f G^0$(298.15), kJ/mole
Zr	25.202	38.869	5.497	0	0

3 Zr–H SYSTEM

3.1 Zr–H System Phase Diagram

At present, the majority of metal-hydrogen binary systems phase diagrams are known [44]. The Zr–H system phase states were among the first to be investigated [24]. The Zr–H system phase diagram is constantly updated, a procedure for the line position (interfaces) calculation on the phase diagram has been elaborated well [45].

As of today, four phases are considered to be the equilibrium phases (Fig. 4) [46 - 50]: hydrogen solid solution in close-packed hexagonal α-Zr; hydrogen solid solution based on high-temperature body-centered cubic phase β-Zr; nonstoichiometric dihydride δ-ZrH_{2-y} with a face-centered cubic (FCC) Zr sublattice; and dihydride ZrH_{2-x} with a tetragonal (FCT, c/a < 1) lattice, with a homogeneity area extending up to the stoichiometric composition (x = H/Zr = 2). The ε-phase forms from the δ- phase at the δ-hydride martensitic transformation [50]. The High-temperature β-Zr phase is in the eutectoid equilibrium with α-Zr(H) and δ-ZrH_{2-y} at a point position: T = 547 °C and x = 0.5. Besides, under certain conditions, a metastable γ-phase with a tetragonal (FCT, c/a>1) lattice is formed which dissociates into α-Zr + δ-ZrH_{2-y} with a temperature rise up to 255 °C [46].

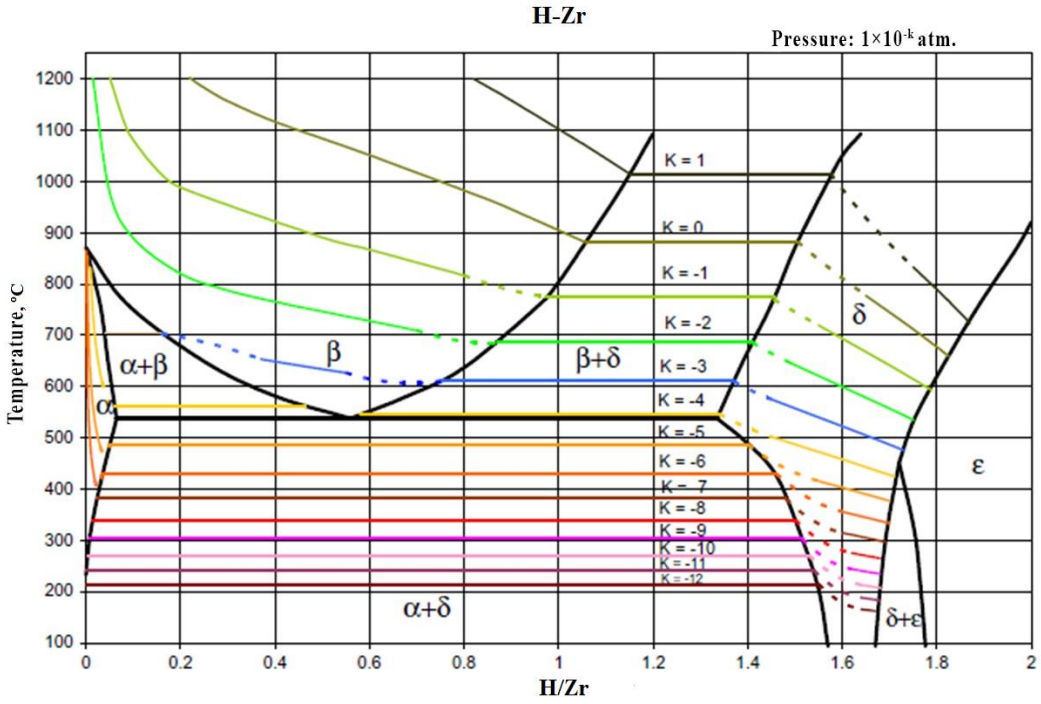

Fig. 4. Zr-H Phase Diagram [46]

Crystallographic data on the Zr–H systems phases are given in Table 8.

Depending on the influence on the polymorphic transformation in Zr, all of the alloying elements and additives are subdivided into α- and β- stabilizers. Hydrogen refers to very strong β-stabilizers – with an increase in hydrogen concentration, the α→β transition temperature decreases from 863 °C for unalloyed Zr to ~ 547 °C with a hydrogen concentration in Zr of ~ 6 at.% [48 - 49].

Table 8

Crystallographic Data

Phase	Formula	Structure	Pearson Symbol	Space Group	Point Group	Lattice Parameters
α-Zr	Zr	FCC	hP2	$P6_3/mmc$ (№194)	D^1_{ch}; 6/mmm	a = 0.3232 nm; c = 0.5147 nm [41]
β-Zr	Zr	BCC	cI2	$Im\bar{3}m$ (№229)	O^9_h; $m\bar{3}m$	0.36090 nm at 862 °C, 0.35453 nm at 20 °C [42]
δ	$ZrH_{1.66}$	FCC	cF14	$Fm\bar{3}m$ (№225)		0.4781 nm [41]
ε	ZrH_2	FCT	tI6	I4/mmm (№139)	D_{4h}; 4/mmm	a = 0.3520 nm; c = 0.4450 nm [41]
Metastable Phases						
γ	ZrH	FCT	tP6	–	–	a = 0.3520 nm; c = 0.4450 nm [41]

Zr saturation with hydrogen at a temperature slightly lower than that of the α→β-transition (for example, at 800 °C) results in concentration transformation, being a transition from α to a two-phase (α+β)-field with subsequent transition to a single-phase β-field at further increase in hydrogen content [51].

In α-Zr, thermal solubility of hydrogen is very low, it is ~6 at. % (~600 ppm[1]) at the eutectoid transformation temperature and it decreases rapidly with decreasing temperature (Fig. 5) [45]. At room temperature, solubility of hydrogen α-Zr does not exceed 1 ppm [48].

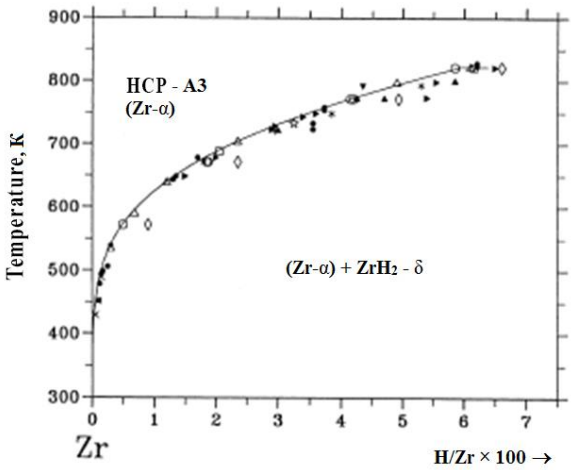

Fig. 5. Thermal solubility of hydrogen in α-Zr [45]

Kearns [52] has systematized and analyzed the data on thermal solubility of hydrogen in Zr, obtained from investigations of hydrogen absorption and diffusion in zirconium under isothermal conditions. He obtained the following equation, describing the temperature dependence of hydrogen on the boundary α/α+δ($C_H^{\alpha/\alpha-\delta}$):

$$C_H^{\alpha/\alpha-\delta}(ppm) = 1.61 \cdot 10^5 \exp(-37447/RT), \quad (5)$$

where $C_H^{\alpha/\alpha-\delta}$ is the concentration of hydrogen on the boundary α/α+δ (ppm); A and B are constants; *R* is the gas constant (R = 8.314462 J/(mole·K)).

In a high-temperature β-Zr (BCC), up to ~ 50 at.% of hydrogen dissolves [48].

Systematization and critical analysis of the isothermal absorption curves with empirical fitting of line positions on the phase diagram was done by Zuzek et al. [48], [49].

Great attention is being paid to creation of data bases for thermodynamic description of phases and Zr–H system phase diagram calculation which was well reported for the Zr–H system in [45]. For description of thermodynamic state of solid solutions and zirconium hydrides, the sublattice Hillert and Staffansson model is used [53], where solid solutions of hydrogen in zirconium are considered as compounds with two sublattices, one being filled

[1]Hereinafter, except where otherwise specified, ppm-part per million.

completely with metal atoms, and the other one – with interstitial atoms (H) and vacancies, designated V_H. The calculation methods used in [45] and thermodynamic parameters of phases that are formed in the Zr–H system are normally taken as a basis for thermodynamic calculations [54].

As noted above, the basic information for plotting a phase diagram is the data on hydrogen absorption.

3.2 Hydrogen Absorption By Zirconium

Hydrogen absorption (dissolution, occlusion) by metal is hydrogen transition from H_2 into metal. The term "absorbed hydrogen" means all absorbed hydrogen contained both in solid solution, and in hydrides. Solubility is a hydrogen concentration limit in solid solution. Hydrogen capacity is a maximum amount of hydrogen that can be absorbed by the metal under consideration.

The process of hydrogen absorption includes stages as follows:

- molecular hydrogen approaches the surface;
- accumulation of hydrogen molecules on the surface and their dissociation (physical adsorption, dissociation and chemical adsorption (chemisorption) of hydrogen molecules);
- relocation of hydrogen atoms by volume (diffusion);
- formation of hydrides upon reaching the hydrogen solubility limit in the hydride-forming metals, such as zirconium.

3.2.1 Hydrogen Adsorption on Zirconium

The basic reactions on gas/metal surface are shown in Fig 6.

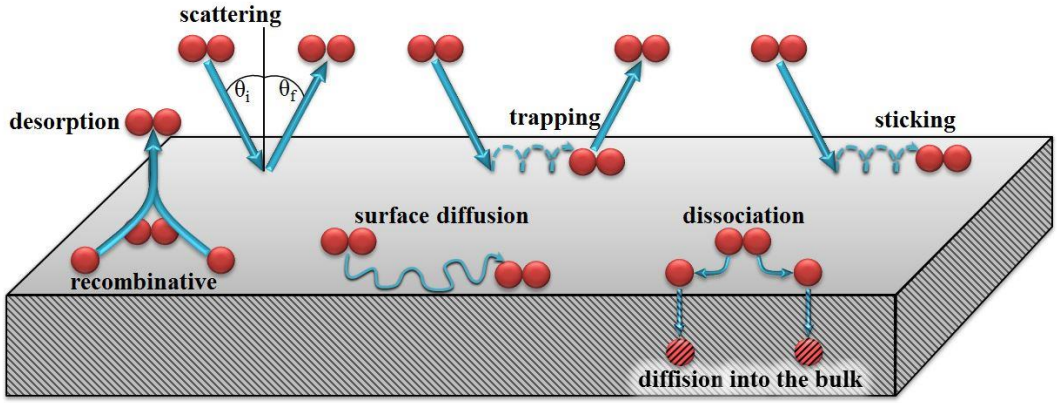

Fig. 6. Reactions on gas/surface surface

Adsorption reaction:

$$H_2 + 2\ (two\ adsorption\ points) \leftrightarrow 2H_{ad}. \quad (6)$$

It should be noted, that there are no special forces which induce adsorption [55]. Hydrogen molecules adsorption on a solid body surface occurs at the expense of hydrogen atoms attraction by adsorbent surface atoms. Gas molecules can be adsorbed on the surface both at the expense of physical and chemical adsorption. Physical adsorption is based on the Van der Waals bond between molecular hydrogen and atoms. In this process, a hydrogen molecule interacts with several adsorbent atoms. The potential energy of a molecule is minimal at the distance of about one radius of an adsorbate molecule (0.2 nm) [12], [56]. The energy of physical adsorption is normally negative; its value in modulus does not exceed 20 kJ/mole H (-0.2 eV). For many metals, the physical adsorption energy is close to -5 kJ/mole H (-0.05 eV) [12]. Since the interaction is weak, a significant physical adsorption takes place only at low temperatures (< 273 K) [56], [57].

Another stage of metal-hydrogen (M–H) reaction: a hydrogen molecule dissociates, and atomic hydrogen overcomes the energy barrier. This process is known as chemisorption. Its energy is normally negative, and the values are from -20 to -400 kJ/mole H. For many metals and for carbon, the chemisorption energy is close to -50 kJ/mole H [12].

Upon dissociation and overcoming the energy barrier, hydrogen atoms diffuse into the bulk.

A diagram representation of the molecular hydrogen potential energy, and the reactions of interaction between molecular and atomic hydrogen with metal atoms is shown in Fig.7 [58].

Zirconium belongs to the metals featuring very active chemical adsorption [59], [60]. Naito [60] determined by kinetic parameters of hydrogen adsorption, that the hydrogen adsorption energy on polycrystalline α-Zr equals -2.84 eV; the bonding force of subsurface layer atoms with their surroundings only slightly differs from the surface atoms bonding force (the bonding energy difference makes only 0.06 eV); the activation energy for adsorption of hydrogen atoms equals -0.02 eV, the energy of atomic diffusion to the bulk equals 0.475 eV. The obtained results demonstrate that hydrogen penetrates zirconium easily, and the process of hydrogen adsorption by zirconium is controlled by the volume diffusion of hydrogen atoms. According to the theoretical estimates reported in [61], the

enthalpy of hydrogen chemisorption on zirconium in both the tetrahedral and octahedral voids for the two surface layers is equal to -3.00 eV.

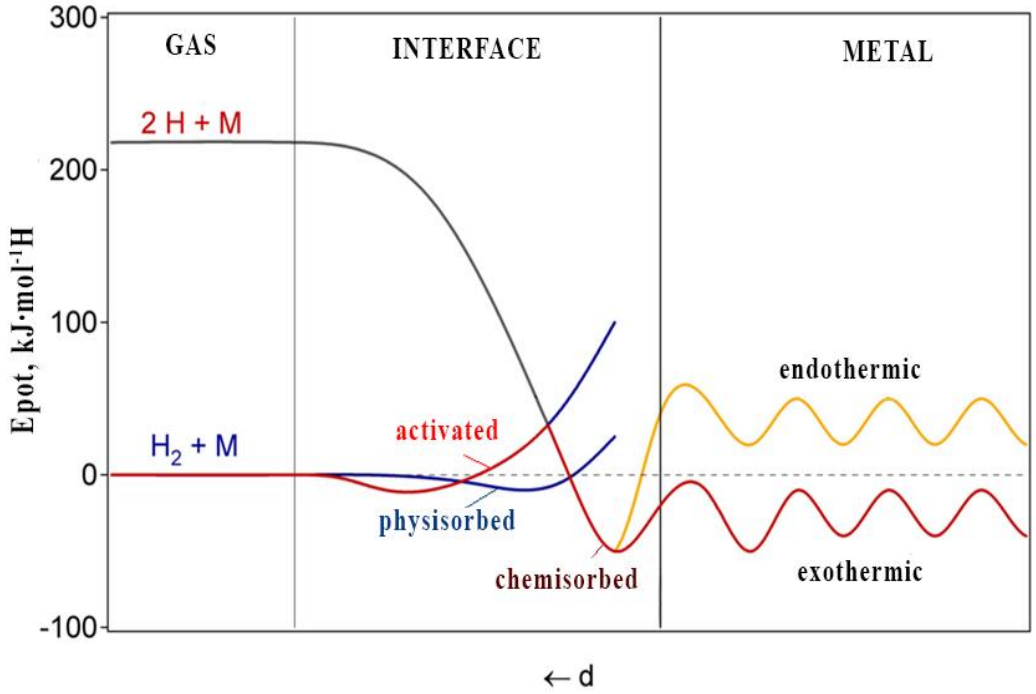

Fig. 7. Diagram of molecular and atomic hydrogen potential energy and reactions, and potential energy of atomic hydrogen with metal atoms. At the physical adsorption, the interaction is determined by the Van der Waals forces. Before the volume diffusion, H_2 dissociates to create an adsorbed state [12], [58]

In accordance with a theoretical evaluation performed by P. Zhang and his colleagues [61], the process of adiabatic dissociation in the H_2/Zr(0001) system has a low barrier (0.05 eV) along the almost stable energy channels; the dissociation of H_2 molecules into atoms takes place at a distance of 0.2 nm over the Zr (0001) surface.

The initial stages of hydrogen interaction with the Zr $(10\bar{1}0)$ surface at 100, 293 and 370 K were investigated by P. Zhang and his colleagues [62] using the NRA (NRA –Nuclear reaction analysis), AES (AES –Auger electron spectroscopy), work function measurements and SSIMS (SSIMS –static secondary ion mass spectroscopy) methods. According to the results obtained, the coefficient of hydrogen attachment to Zr$(10\bar{1}0)$ surface at 100, 293 and 370 K is 1; 0.71 and 0.5, respectively. The hydrogen concentration on the surface first rapidly increases, and then passes into saturation. The surface barrier height is 42.3 kJ/mole which corresponds to the energy of hydrogen diffusion to volume.

Zhang and his colleagues studied the segregation of H and D to Zr(0001) surface using the NRA, WF, AES and SIMS methods; determined 194 °C (467 K) to be the maximum segregation temperature [63]. It was established that at the temperatures up to 194 °C, in the samples with a 59 ppm hydrogen content, hydrogen diffuses from volume to surface (hydrogen segregation on Zr (0001) surface takes place with formation of small hydride-like precipitates), while at higher temperatures, hydrogen moves from surface to volume.

α-Zr (HCP) has a lower value of hydrogen atomic recombination constant as compared to those of the FCC (Ni) and BCC (Al, Fe) metals [64].

Because of the insignificant values of hydrogen atom enthalpy on surface and in subsurface layer, the process of recombination and subsequent desorbtion of hydrogen atoms in H_2/Zr system at the temperature of ~ 400 K is practically excluded [62].

3.2.2 Kinetics of Hydrogen Absorption By α-Zr

Among the transition metals, the best absorbents are the first members, with their d-zone being less than half filled [65]. As the d-zone of a metal is filled with electrons, its absorption capacity decreases. Palladium is an exception, its atoms contain 10 d-electrons, but it is a good absorbent. In full conformity with this mechanism, zirconium easily absorbs hydrogen (Fig. 8) [66 - 69].

The kinetics of hydrogen absorption by zirconium (variation in the quantity of hydrogen accumulated with time, at prescribed time and pressure) was studied in [70 - 72]. In the majority of works, it is reported that the quantity of hydrogen absorbed by α-Zr, varies with time according to the parabolic law:

$$C_H{}^2 = k_{ab}t, \tag{7}$$

where C_H – is the quantity of absorbed hydrogen, k_{ab} – is the parabolic velocity constant:

$$k_{ab} = k_0 exp\left(\frac{-E_{ab}}{RT}\right), \tag{8}$$

where E_{ab} – is the energy of the reaction of hydrogen absorption by α-zirconium.

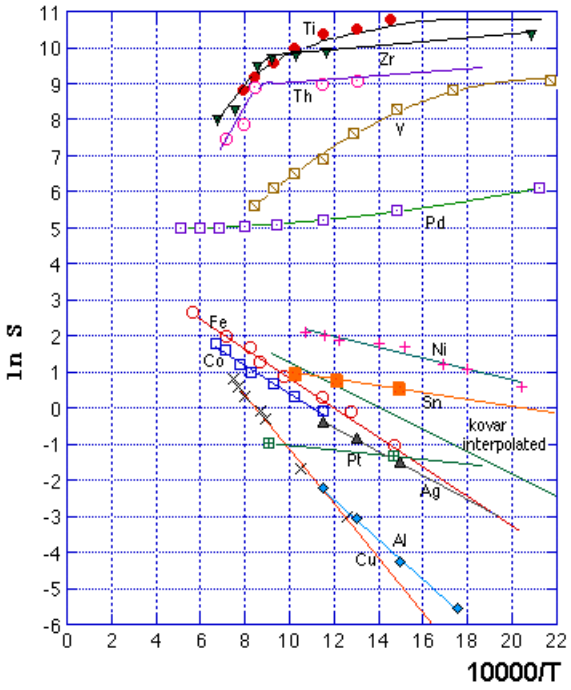

Fig. 8. lnS (S – amount of hydrogen in cm^3 capable of absorbing 100 g of metal at 1 atm) versus temperature [69]

According to [71], in the temperature range of 250…425°C, and at the pressure of 1 atm., the reaction of hydrogen absorption by zirconium follows the parabolic law; parabolic velocity constant [(ml/cm^2)^2 per second] is calculated by the equation:

$$k_{ab} = 2.3 \cdot 10^5 exp\left(\frac{-71964.8 \pm 836.8}{RT}\right), \quad (9)$$

where R – is the gas constant (R = 8.31467 J/(mole·K)), and (71.9648±0.8368) kJ/mole – the reaction energy of hydrogen absorption by α-Zr.

Certain changes in the absorption kinetics can be caused by the surface condition and oxidation during hydrogenating [72].

Dependence of the rate of hydrogen absorption by zirconium (at the initial hydriding stage) passes through maximum at 500 °C [73].

With an increase of hydriding time, the amount of absorbed hydrogen passes into saturation.

At a given pressure, the absorption capability of zirconium decreases with increasing temperature (see Fig. 8) [66 - 69], which is characteristic of all exothermic reactions (the enthalpy of hydrogen dissolution by zirconium is negative).

Under atmospheric pressure and at the temperature of 20°C, the ultimate quantity of hydrogen absorbed by zirconium equals to 240 cm^{3}of hydrogen per 1 g of zirconium. At 400, 800 and 1100°C, this value is equal to 235, 160 and 40 cm^3/g, respectively [67].

The optimal zirconium hydriding temperature is 300…400 °C [66].

Unlike nitrogen and oxygen, almost all of the absorbed hydrogen can be removed from zirconium at its heating in vacuum to 1000…1200 °C [66].

3.2.3 Thermodynamics of Absorption

3.2.3.1 General Provisions

Judging by the character of chemical bonding, according to accepted classification, all M-H (metal-hydrogen) compounds are subdivided into three main classes:

- ionic hydrides (salts);
- metal hydrides;
- covalent hydrides (molecular compounds).

In full conformity with Zr position in the periodic table (Fig.9), zirconium hydrides refer to metal hydrides [37].

Investigations on metal structure changes at hydriding indicate [74] that insertion of a hydrogen atom in a metal lattice can:

- be followed by a fundamental metal lattice rearrangement, or in other words, changing the type of packing of metal atoms, e.g., transition from the body-centered cubic (BCC) packing in the individual metal structure to the side-centered cubic packing (FCC) in the hydride metal sublattice;
- not result in essential changes in metal structure. In this case, metal atoms packing in the hydride metal sublattice is no different from the packing in the individual metal structure, or only an insignificant deformation of the unit cell of the lattice occurs.

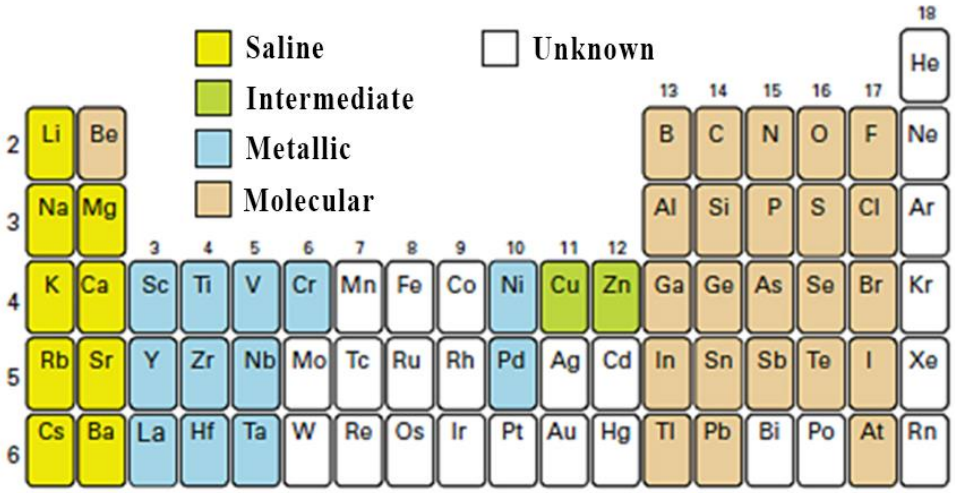

Fig. 9. Position of zirconium in the periodic table

Hydrogen penetration in zirconium lattice upon reaching thermal solubility results in a metal lattice rearrangement (HCP) and formation of hydrides with a different structure (FCC, FCT) [8].

Depending on the thermal effect symbol, there are distinguished the endothermal (with absorption of heat) and exothermal (with heat release) absorptions. The metals, which absorb hydrogen following the endothermal reaction (aluminium, cuprum, ferrum, etc.) do not form hydrides. The metals, which absorb hydrogen following the exothermal reaction (titanium, zirconium, vanadium, niobium, tantalum), form hydrides upon reaching the solubility limit. The absorption symbol (reaction type) is associated with the position in the periodic table: all metals located to the left of Cr, dissolve hydrogen according to the exothermal reaction, the metals located to the right of Cr, follow the endothermal reaction [75].

Dissolution enthalpy changes in 3d, 4d and 5d transition metals is presented in Fig. 10 [76].

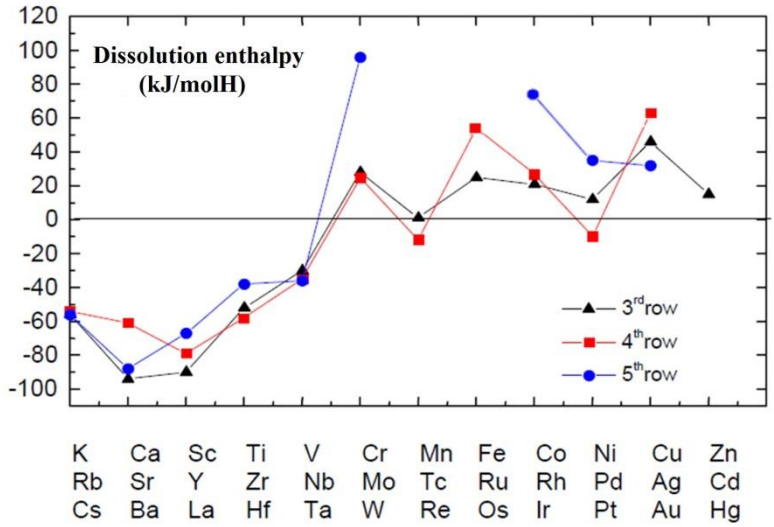

Fig. 10. Dissolution enthalpy changes in 3d, 4d and 5 transition d-metals [76]

The thermodynamic equilibrium in metal-hydrogen (M–H) system is normally represented by the pressure-composition-temperature (P-C-T) diagram (pressure-composition isotherm). Normal view of the pressure-composition isotherm is shown in Fig 11.

The initial sharp rise of the curve corresponds to hydrogen dissolution in the initial phase (normally designated as α). In this area (up to the solubility limit), hydrogen dissolution takes place without significant changes of α-lattice, and the dependence of hydrogen concentration (C_H) on pressure is described by Sieverts's law:

$$C_H^\alpha = K_H^\alpha \sqrt{P_{H_2}}, \tag{10}$$

where K_H– is the Sieverts's constant (constant of hydrogen dissolution in α-phase); C_H^α– is the hydrogen concentration in solid solution; P_{H_2}– is the hydrogen pressure over metal.

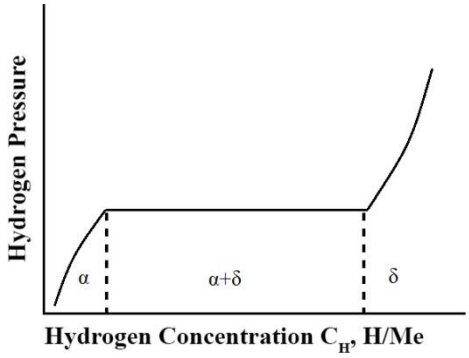

Fig. 11. Pressure-Composition isotherm. Upon reaching solubility limit in α-phase, hydride formation begins from the α-phase supersaturated solid solution [57]

Temperature dependence of equilibrium pressure over metal at the stage of hydrogen dissolution in the initial phase solid solution is described by the equation:

$$\frac{1}{2} ln \frac{P_{H_2}}{P_0} = \frac{\Delta H_S}{RT} - \frac{\Delta S}{R}, \tag{11}$$

where P_0 – is the reference pressure (1 atm).

The enthalpy of hydrogen dissolution in α-ZrΔH_S = -58 kJ/mole·H (-0.601 eV) [76].

Upon reaching the hydrogen solubility limit in α-phase, hydride formation begins. With appearance of the second phase (hydrides, that are normally designated β in the thermodynamic description of M-H system), the pressure over the material being hydrided which is in equilibrium with the solid solution internal pressure), does not change, and further increase in the amount of absorbed hydrogen is not accompanied by a pressure increase (α→β-transition region). The hydrogen concentration in each phase remains constant, however, the volume fraction of each of the phases changes. The equilibrium pressure of hydride formation (α(H_x)→α+β) is described by the Van't Hoff equation [12], [56 - 57]:

$$ln \frac{P_{eq}}{P_0} = \frac{\Delta H_f}{RT} - \frac{\Delta S_f}{R}, \tag{12}$$

where P_{eq} – is the hydrogen pressure over metal in the two-phase field α-β (on the plateau, Fig. 11, Fig. 10), ΔH_f and ΔS_f– are the enthalpy and entropy of hydride formation.

If we plot the logarithm of hydride formation versus 1/T, we get a line (Van't Hoff plot) as shown in Fig 12. The activation energy of hydride formation from the oversaturated solid solution α is determined from the slope of this plot.

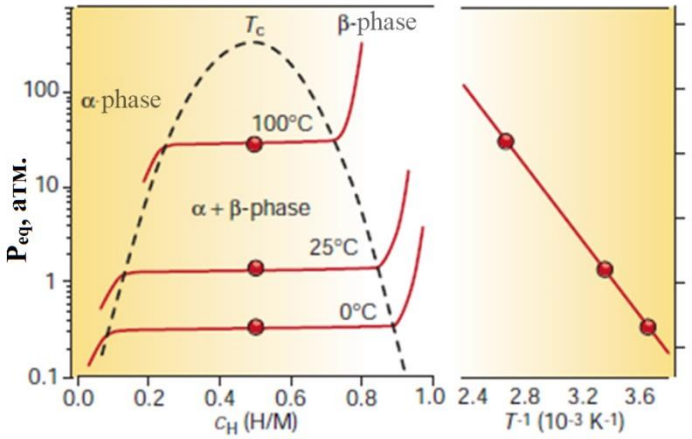

Fig. 12. P-C-T diagram and Van't Hoff plot: α– solid solution of hydrogen in α-phase; β–hydride; α + β– two-phase field [12], [56 - 57]

Since entropy change is essentially determined by the change in hydrogen state from the molecular gaseous state to the dissociated in absorbed state, and that is practically the standard hydrogen entropy (S_0= 130 J/mole H_2×K), therefore, $\Delta S_f \approx$ -130 J/mole H_2·K for all M–H systems [12], [56].

The most stable metallic hydrides, for example, HoH_2, have the enthalpy of formation ΔH_f = -226 kJ/mole H_2. The least stable hydrides are $FeH_{0.5}$; $NiH_{0.5}$ and $MoH_{0.5}$ with the enthalpy of formation ΔH_f = +20 kJ/mole H_2, ΔH_f = +20 kJ/mole H_2 and ΔH_f = +92 kJ/mole H_2, respectively [56].

Upon completion of the α -β transition, dissolution hydrogen in hydride (β) takes place.

Sometimes, the pressure-composition isotherm has a number of plateaus, which indicate that during hydrogen absorption, M–H system undergoes several two-phase stages.

3.2.3.2 Thermodynamics of Hydrogen Absorption By Zirconium

The P–C–T diagrams for Zr–H system are shown in Fig. 13 [48]. Below the eutectic temperature (550 °C), hydrogen concentration in zirconium increases proportionally to $p^{1/2}$, which corresponds to hydrogen dissolution in solid solution α-Zr:

$$C_H^{\alpha-Zr} = K_H^{\alpha-Zr}\sqrt{P_{H_2}} \quad (13)$$

Temperature dependence of the Sieverts constant for hydrogen dissolution in α-Zr is described by the equation [48]:

$$K_H^{\alpha-Zr}(T)\left\{\frac{[H]}{[M]}(torr)^{-\frac{1}{2}}\right\} = 7.854\cdot 10^{-5}\exp\left(\frac{6481}{T}\right). \quad (14)$$

Further there is a plateau, corresponding to the two-phase field α + δ.

Temperature dependence of the equilibrium pressure at formation of δ-hydrides in α-Zr [48]:

$$P_{eq}^{\alpha+\delta}(torr) = 6.545\cdot 10^{11}\exp\left(-\frac{24321}{T}\right). \quad (15)$$

After that, the pressure increases again with increase of concentration in the single-phase δ-hydride.

At the temperature ranging between 550 and ~ 750 °C, the absorption isotherms of Zr–H system have two plateaus. One of them corresponds to the two-phase field α + β, and the other – to the two-phase field β + δ. At T > 750 °C, the first plateau, corresponding to the two-phase field α + β, disappears, leaving only the plateau which corresponds to the two-phase field β + δ.

At the temperatures of 900 °C and higher, hydrogen continuously dissolves in β-Zr.

The enthalpy values for different reactions in Zr-H system can be obtained by processing the P-C-T curves in accordance with the rules given in Table 9 and in Fig. 14 [78].

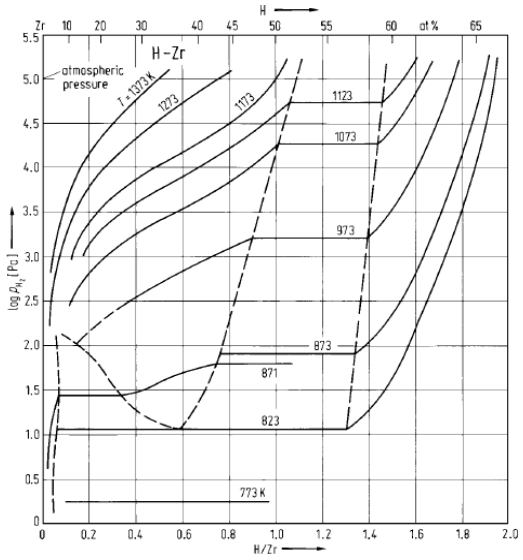

Fig. 13. Pressure-Compossition Isotherm of Zr-H System Zr-H [48]

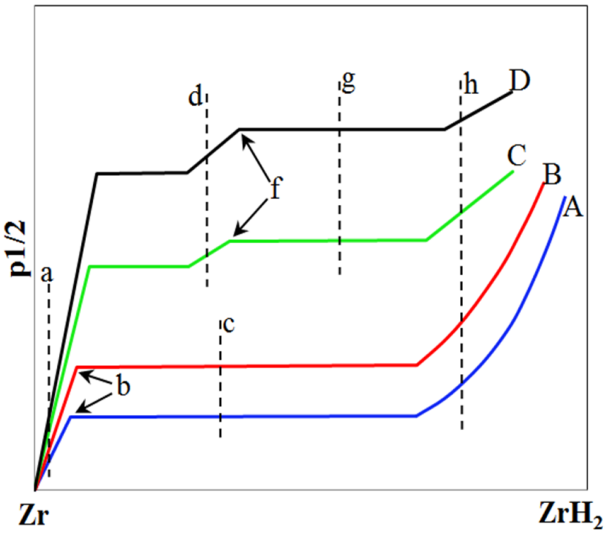

Fig. 14. Pressure-Compossition Isotherms of Zr-H System; T_A<T_B<550 °C<T_C<T_D [78]

The enthalpy of forming δ-hydride ΔH_f^{δ} =-141 kJ/mole δ, the free energy of δ-hydride ΔG_f^{δ} formation = -96.2 kJ/mole δ, the entropy of δ-hydride ΔS_f^{δ} formation = -151J/K·mole δ [48].

Yao and Wang, and colleagues [79] investigated hydrogen absorption and desorption at 360 °C for the cycle: H_2 absorption during 1 hour at 4 MPa / desorption during 1 hour at 0.01 MPa, and found that under such conditions, the unalloyed α-Zr absorbs hydrogen easily and rapidly, while the desorption takes place very slowly: α-Zr hydrogen absorption rate at 4 MPa equals 0.044 [H]/[M]×s^{-1}, its desorption rate at 0.01 MPa is 0.007 [H]/[M]×s^{-1}.

The full energy of hydrogen emission from δ-hydride = 144.7 kJ/mole H [80].

The data on the enthalpy of binary hydride formation depending on the metal position in the periodic system are provided in Fig. 15 [81].

Table 9

Thermodynamic Characteristics of Reactions in Zr-H System
(characteristics determined according to P–C–T) [78]

Composition (Fig. 14)	f– function depending on →1/T	Enthalpy = $R\frac{d(f)}{d(1/T)}$		Value of reaction enthalpy, kJ/mole
a	lnP	$\Delta H_s^{\alpha-Zr}$	Enthalpy of dissolving molecular hydrogen H_2 in α-Zr	-101.7…-120.9
b	lnC	$\Delta H_{\alpha+\delta\rightarrow\alpha}$	Enthalpy of dissolving δ-hydride in supersaturated solid solution α-Zr	+36.0
c	lnP	$\Delta H_{\alpha\rightarrow\alpha+\delta}$	Enthalpy of forming δ-hydride from supersaturated solid solution α-Zr	-164.0…-191.6
d	lnP	$\Delta H_s^{\beta-Zr}$	Enthalpy of dissolving molecular hydrogen H_2 in β-Zr	-128.9…-169.5
f	lnC	$\Delta H_{\beta+\delta\rightarrow\beta}$	Enthalpy of dissolving δ-hydride in supersaturated solid solution β-Zr	+9.6
g	lnP	$\Delta H_{\beta\rightarrow\beta+\delta}$	Enthalpy of forming δ-hydride from supersaturated solid solution β-Zr	-205.4…-222.6
h	lnP	$\Delta H_s^{\delta r}$	Enthalpy of dissolving molecular molecular hydrogen H_2 in δ-hydride	-165.3…-188.7

Group	1	2	3	4	5	6	7	8	9	10	11	12	13	14	15	16	17	18
Period																		
1	H_2 -																	He -
2	LiH -176												BH_3 -	CH_4 -	NH_3 -	OH_2 -	FH -	Ne -
3	NaH -117	MgH_2 -75											AlH_3 -	SiH_4 -	PH_3 -	SH_2 -	ClH -	Ar -
4	KH -117	CaH_2 -176	ScH_2 -201	TiH_2 -126	VH -59	CrH -17	MnH -17	FeH 33	CoH 33	NiH 17	CuH -	ZnH_2 -	GaH_3 -	GeH_4 -	AsH_3 -	SeH_2 -	BrH -	Kr -
5	RbH -109	SrH_2 -188	YH_2 -226	ZrH_2 -164	NbH -76	MoH 17	TcH 50	RuH 67	RhH 38	PdH -33	AgH -	CdH_2 -	InH -	SnH_4 -	SbH_3 -	TeH_2 -	IH -	Xe -
6	CsH -100	BaH_2 -176	LaH_2 -209	HfH_2 -134	TaH_2 -59	WH 42	ReH 92	OsH 84	IrH 67	PtH 17	AuH -	HgH_2 -	TiH -	PbH_4 -	BiH_3 -	PoH_2 -	AtH -	Rn -
Lan.				CeH_2 -205	PrH_2 -209	NdH_2 -209		SmH_2 -222	EuH_2 -	GdH_2 -201	TbH_2 -	DyH_2 -	HoH_2 -	ErH_2 -226		YbH_2 -		
Act.				ThH_2 -146		UH_3 -84		PuH_2 -155										

Fig. 15. Enthalpy of Binary Hydrides Formation, kJ/moleH_2 [81]

REFERENCES

1. IAEA-TECDOC-1410. *Delayed hydride cracking in pressure tube nuclear reactors*. International Atomic Energy Agency, Vienna. 2004.

2. IAEA-TECDOC-1649. *Delayed hydride cracking of zirconium alloy fuel cladding*. International Atomic Energy Agency, Vienna. 2010.

3. C.K. Chao, K.C. Yang, and C.C. Tseng. *Rupture of spent fuel zircaloy cladding in dry storage due to delayed hydride cracking* // Nuclear Engineering and Design.2008,vol. 238,№1, p. 124-129.

4. Y. Fukai. *The metal-hydrogen system. Basic bulk properties*. Series: Springer Series in Materials Science. vols. 21. 2nd rev. and updated ed. 2005, XII, 497 p.

5. E. Y. Afanasieva, I. A. Evdakimov, O. V. Khoruzhii, V. V. Likhanskii, and A. A. Sorokin. *Modeling of fuel rods hydriding failures in water reactors*. Transactions of the 17th International Conference on Structural Mechanics in Reactor Technology (SMiRT 17). Praque. Chech Republic. August 17-22. 2003, Paper # C03-1.

6. Anna-Maria Alvarez Holston. *In-pile and out-of pile methods to predict fuel cladding failures*. SCIP Property Information. Studvik. October 2011.

7. R.M. Lobo, A.H.P. Andrade, and M. Castagnet. *Hydride embrittlement in zircaloy components*. International Nuclear Atlantic Conference - INAC 2011. Belo Horizonte. MG. Brazil. October 24-28. 2011, Associacao Brasileira De Energia Nuclear - Aben. ISBN: 978-85-99141-04-5.

8. M. P. Puls. *The effect of hydrogen and hydrides on the integrity of zirconium alloy components* // Engineering materials, 2012.

9. R. A. Andriyevskiy, Ya. S. Umanskiy. *Interstitial Alloys*. M.: Main Office of Physico-Mathematical Literature «Science», 1977.

10. R.A. Andriyevskiy. *Materials Science of Hydrides*. M.: «Metllurgy»,1986.

11. W. Grochala and P. P. Edwards. Thermal decomposition of the non-interstitial hydrides for the storage and production of hydrogen // *Chemical Reviews*. 2004, vol. 104, №3, p. 1283-1315.

12. A. Zuttel, A. Borgschulte, and L. Schlapbach. *Hydrogen as a future energy carrier*. WILEY-VCH Verlag GmbH & Co. KGaA. Weinheim. 2008.

13. W. Pearson. *Crystal Chemistry and Physics of Metals and Alloys* (Science & Technology of Materials) Part. I / Transl. from Engl. S. N. Gorina. M.: «Mir», 1977.

14. A. Niederberger. Updating the size of the proton: small difference. big consequence // *Optics and Photonics Focus*. 26 August 2010, vol. 10, story 4.

15. J.E. Sansonetti and W.C. Martin. Handbook of basic atomic spectroscopic data // *Journal of Physical and Chemical Reference Data*. 2005, vol. 34, №4, p. 1559-2259.

16. K. Christmann. Interaction of hydrogen with solid surfaces //*Surface Science Reports*. 1988, vol. 9, №1-3, p. 1-163.

17. K.R. Lykke, K.K. Murray, and W.C. Lineberger. Threshold photodetachment of H^- // *Physical Review A*. 1991, vol. 43, №11, p. 6104-6107.

18. J.C. Rienstra-Kiracofe, G.S. Tschumper, and H.F. Schaefer.Atomic and molecular electron affinities: photoelectron experiments and theoretical computations // *Chemical Reviews*. 2002, vol. 102, №1, p. 231-282.

19. H. Lu, D. Dai, P. Yang, and L. Li. Atomic orbitals in molecules: general electronegativity and improvement of Mulliken population analysis // *Physical Chemistry. Chemical Physics*. 2006, vol. 8, №3, p. 340-346.

20 R.B. McLellan and C.G. Harkins. Hydrogen interactions with metals // *Materials Science and Engineering*. 1975, vol. 18, №1, p. 5-35.

21 Yu-Ranl Luo and S. Benso. The covalent potential: a simple and useful measure of the valence-state electronegativity for correlating molecular energetics // *Account of Chemical Research*. 1992, vol. 25, p. 375-381.

22. P.K. Mandal and E. Arunan. Hydrogen bond radii for the hydrogen halides and van der Waals radius of hydrogen // *The Journal of Chemical Physics*. 2001, vol. 114, №9, p. 3880-1…3880-3.

23. P. Rodriguez and V. S. Arunachalam.Influence of interstitials on the mechanical properties of group IV b metals // *In: Symposium on Non-ferrous Metals Technology. Volume III - Nickel. Lead. Zinc. Rare earth and Nuclear Metals*. NML. Jamshedpur. Jamshedpur. 1969. eprints.nmlindia.org/3926/.

24. Kh.D. Goldshmidt. *Interstitial Alloys*. №II. M.: «Mir», 1971.

25. R.D. Shannon and C.T. Prewitt.Effective ionic radii in oxides and fluorides // *Acta Crystallographica B*. 1969, vol. B25, №5, p. 925-945.

26. D.W. Chakeres. Harmonic quantum integer relationships of the fundamental particles and bosons // *Particle Physics Insights*. 2009; 2: p. 1-20.

27. L. Pauling. The application of the quantum mechanics to the structure of the hydrogen molecule and hydrogen molecule-ion and to related problems // *Chemical Reviews*. 1928, vol. 5, №2, p. 173-213.

28. Yu. A. Velikov. Interatomic Interaction and Electronic Structure of Solids // *Soros Educational Journal*. 1996, №11, p. 80-86.

29. O. N. Temkin. Molecular Hydrogen Chemistry// *Soros Educational Journal*. 2000, vol. 6, №10, p. 31-36.

30. R. Griessen. *The lecture "Science and technology of hydrogen in metals". X Chapter: Safety*. Vrije Universiteit. Amsterdam. 2008.

31. Chang-Guo Zhan, J.A. Nichols, and D.A. Dixon. Ionization potential. electron affinity. electronegativity. hardness. and electron excitation energy: molecular properties from density functional theory orbital energies // *The Journal of Physical Chemistry A*. 2007, vol. 107, №20, p. 4184-4195.

32. L. Pichl, Y. Li, R.J. Buenkerm and M. Kimura. Electronic potential energy of H^{-2} and CHe^{4+} diatomic ions // *Journal of Plasma and Fusion Research Series*. 2006, vol. 7, p. 249-252.

33. M.W. Chase, Jr. NIST - JANAF Thermochemical tables. Fourth Edition. Part I - II // *Journal of Physical and Chemical Reference Data*. Monograph №9, 1998, p. 1-1951.

34. C.S. Feigerle, R.R. Corderman, S.V. Bobashev, and W.C. Lineberger. Binding energies and structure of transition metal negative ions // *Journal of Chemical Physics*. 1981, vol. 74, №3, p. 1580-1598.

35. A.L. Allred. Electronegativity values from thermochemical data // *Journal of Inorganic and Nuclear Chemistry*. 1961, vol. 17, №3-4, p. 215-221.

36. W. Gordy and W.J.O. Thomas. Electronegativities of the elements // *The Journal of Chemical Physics*. 1956, vol. 24, №2, p. 439-443.

37. R. Griessen. *The lecture "Science and technology of hydrogen in metals". IX Chapter: Sustainability and hydrogen*. Vrije Universiteit. Amsterdam. 2008.

38. S. Banerje and P. Mukhopadhyay. Phase transformations on examples from titanium and zirconium // *Pergamon Materials Series*. 2007, vol. 12. p. 1-813.

39. L.T. Bugayenko, S.M. Ryabyh and A.L. Bugayenko. Almost complete system of ionic crystallographic radius Midradiuses and its use to determine ionization potentials // *Bulletin of Moscow University*, Series 2. Chemistry. 2008, vol. 49, №6, p. 363-383.

40. S.J. Liu,. S.Q. Shi, H. Huang, and C.H. Woo. Interatomic potentials and atomistic calculations of some metal hydride // *Journal of Alloys and Compounds*. 2002, vol. 330-332, p. 64-69.

41. R.M. Daum, Y.S. Chu, and A.T. Motta. Identification and quantification of hydride phases in zircaloy-4 cladding using synchrotron X-ray diffraction // *Journal of Nuclear Materials*. 2009, vol. 392, №3, p. 453-463.

42. R.B. Russell. Coefficients of thermal expansion for zirconium // *Transactions AlME. Journal of Metals*. September 1954, p. 1054-1052.

43. *Thermophysical properties of materials for nuclear engineering: Tutorial for students of specialty Nuclear power plants* / Edited by Prof. P.L. Kirillov. 2nd revised and augmented edition. Obninsk. 2006, 182 p.

44. J.R. Davis. *ASM Handbook*, vol. 3 Alloy phase diagrams. 1992, p. 1-1471.

45. N. Dupin, I. Ansara, C. Servant, C. Toffolon, C. Lemaignan, and J. C. Brachet. A thermodynamic database for zirconium alloys // *Journal of Nuclear Materials*. 1999, vol. 275, №3, p. 287-295.

46. K.A. Terrani, M. Balooch, D. Wongsawaeng, S. Jaiyen, and D.R. Olander.The kinetics of hydrogen desorption from and adsorption on zirconium hydride // *Journal of Nuclear Materials*. 2010, vol. 397, №1-3, p. 61-68.

47. E. Tulk, M. Kerr, and M. R. Daymond. Study on the effects of matrix yield strength on hydride phase stability in zircaloy-2 and Zr 2.5 wt% Nb // *Journal of Nuclear Materials*. 2012, vol. 425, №1-3, p. 93-104.

48. E. Zuzek, J.P. Abriata, A. San-Martin, and F.D. Manchester.T he H - Zr (Hydrogen - Zirconium) system // *Bulletin of Alloy Phase Digrama*. 1990, vol. 11, №4, p. 385 -395.

49. E. Zuzek. On equilibrium in the Zr-H system // *Surface and Coatings Technology*. 1986, vol. 28, №3-4, p. 323-338.

50. I.O. Bashkin, M.F. Nefedova and V.G. Tissen. Superconductivity in Zr - D system under pressure // *Solid-State Physics*. 2000, vol. 42, №1, p. 12-15.

51. E. Hong, D.C. Dunand and H. Choe. Hydrogen-induced transformation superplasticity in zirconium // *International Journal of Hydrogen Energy*. 2010, vol. 35, №11, p. 5708-5713.

52. J.J. Kearns. Terminal solubility and partitioning of hydrogen in the alpha phase of zirconium, Zircaloy-2 and Zircaloy-4 // *Journal of Nuclear Materials*. 1967, vol. 22, №3, p. 292-303.

53. M. Hillert and L.-I. Staffansson. The regular solution model for stoichiometric phases and ionic melts // *Acta Chemica Scandinavica*. 1970, vol. 24, №10, p. 3618-3626.

54. Y. Zhong and D.D. Macdonald. Thermodynamics of the Zr-H binary system related to nuclear fuel sheathing and pressure tube hydriding // *Journal of Nuclear Materials*. 2012, vol. 423, №1- 3, p. 87-92.

55. T.M. Roshchina. Adsorption phenomena and surface // *Soros Educational Journal*. 1998, №2, p. 89-98.

56. A. Zuttel. Materials for hydrogen storage // *Materials Today*. 2003, vol. 6, №9, p. 24-33.

57. M. Dornheim.Thermodynamics of metal hydrides: Tailoring reaction enthalpies of hydrogen storage materials / chapter in *Handbook of hydrogen storage*. edited by M. Hirschler. Wiley-VCH(2010), p. 891-918. Head of Department Nanotechnology. Berlin.

58. A. Borgschulte, R.J. Westerwaal, J.H. Rector, H. Schreuders, B. Dam and R. Griessen. Catalytic activity of noble metals promoting hydrogen uptake // *Journal of Catalysis*. 2006, vol. 239, №2, p. 263-271.

59. P. Nordlander, J.K. Norskov, and F. Besenbacher. Trends in hydrogen heats of solution and vacancy trapping energies in transition metals // *Journal of Physics F: Metal Physics*. 1986, vol. 16, №9, p. 1161-1171.

60. M. Yamamoto, S. Naito, M. Mabuchi, and T. Hashino.Adsorptlon potential of hydrogen atom on zirconium // *The Journal Physical Chemistry*. 1992, vol. 96, p. 3409-3412.

61. P. Zhang, S.-X. Wang, J. Zhao, C.-H. He, and P. Zhang. First-principles study of H_2 adsorption and dissociation on Zr (0001) // *Journal of Nuclear Materials*. 2011, vol. 418, №1-3, p. 159-164.

62. C.-S. Zhang, B. Li, and P. R. Norton. The initial stages of interaction of hydrogen with the surface // *Surface Science.* 1996, vol. 346, №1-3, p. 206-221.

63. C.-S. Zhang, B.J. Flinn, and P.R. Norton. Segregation of hydrogen on zirconium (0001) studies by SIMS. work function. Auger electron spectroscopy and nuclear reaction analysis // *Journal of Nuclear Materials*. 1993, vol. 199, №3, p. 231-236.

64. M.I. Baskes.A calculation of the surface recombination rate constant for hydrogen isotopes on metals isotopes on metals // *Journal of Nuclear Materials*. 1980, vol. 92, №2-3, p. 318-324.

65. Yu.M. Dergachev. A Model of hydrogen absorption by metals // *Inorganic materials*. 2009, vol. 45, №8, p. 930-933.

66. G.A. Meyerson and A.N. Zelikman. *Metallurgy of rare metals*. M.: “Metallurgizdat”, 1955.

67. G.L. Miller. *Zirconium* / Translated from the English under the editorship of S. G. Glazunova and A. A. Kiseleva. M.: Foreign Literature, 1955.

68. E.A. Gulbransen and K. F. Andrew. Solubility and decomposition pressures of hydrogen in alpha-zirconium // *Transactions AIME. Journal of Metals*. January 1955, vol. 7, №1, p. 136-144.

69. *REB Research - Hydrogen Solubility In Various Metals* [http://www.rebresearch.com/H2sol2.htm].

70. S. Naito. Kinetics of hydrogen absorption by α-zirconium // *Journal of Chemical Physics*. 1983, vol. 79, №6, p. 3113-3120.

71. J. Belle, B. B. Cleland, and M. W. Mallett. Kinetics of the reaction of hydrogen with zirconium // *Journal of the Electrochemical Society*. 1954, vol. 101, №5, p. 211-214.

72. G. Meyer, M. Kobrinsky, J. P. Abriata, and J. C. Bolcich. Hydriding kinetics of zircaloy-4 in hydrogen gas // *Journal of Nuclear Materials*. 2 April 1996, vol. 229, p. 48-56.

73. J. Park, W. Kim, and M. Won. Hydrogen sorption in zirconium and relevant surface phenomena // *Materials Transactions*. 2007, vol. 48, №5, p. 1012-1016.

74. V.A. Yartys, V.V. Burnasheva, K.N. Semenenko. Structural Chemistry of Hydrides of Intermetallic Bonds // *Academy of Sciences of the USSR*. Sov. Chem. Rev. 1983, vol. LII, №4, p. 529-561.

75. Yu.M. Degtyariov. Hydrogen Absorption by Transition Metals // *Inorganic Materials*. 2006, vol. 42, №2, p. 147-150.

76. R. Griessen. *The lecture "Science and technology of hydrogen in metals". III Chapter: Thermodynamics of hydrogen in metals*. Vrije Universiteit. Amsterdam. 2008.

77. L. Schlapbach and A. Zuttel. Hydrogen-storage materials for mobile applications // *Nature*. 2001, vol. 414, №6861, p. 353 -358.

78. D.G. Westlake. Enthalpy data for the zirconium -hydrogen system // *Journal of Nuclear Materials*. 1962, vol. 7, №2, p. 346-347.

79. M.Y. You, J.H. Wang, J.C. Peng, B.X. Zhou, and Q. Li. Study on the role of second phase particles in hydrogen uptake behavior of zirconium alloys // *Journal of ASTM International Selected Technical Papers STP1529. Zirconium in the Nuclear Industry: 16th International Symposium. ASTM International*. West Conshohocken. 2011, p. 466-483.

80. J.A. Llauger and G.N. Walton. Absorption and desorption of hydrogen from zirconium foil // *Journal of Nuclear Materials*. 1981, vol. 97, p. 185-191.

81. H.H. van Mal. Stability of ternary hydrides and some application // *Philips Research Reports Supplements*. 1976, №1, p. 1-87.

Article received 24.07.2013

ВОДОРОД В ЦИРКОНИИ
Часть 1

Т.П. Черняева, А.В. Остапов

Систематизированы сведения о поведении водорода в цирконии. Предлагаемые материалы касаются ряда основных физико-химических характеристик двух участников реакции взаимодействия Zr–H (H и Zr), а также фундаментальных данных о системе Zr–H в целом. Приводятся сведения о положении атомов водорода в решетке Zr (преимущественно тетрагональные пустоты) и его динамике. Следует отметить, что дискуссионным является вопрос относительно того, имеет ли растворенный в цирконии водород состояние нейтральных атомов H^0 или ионов (H^+, H^-, $H^{\delta-}$, $H^{\delta+}$), в то же время однозначно утверждается, что водород в цирконии не встречается в молекулярном состоянии и не образует пор, заполненных молекулярным газообразным водородом. Изложены основные принципы взаимодействия водорода с металлами (M). Представлена термодинамика адсорбции и абсорбции водорода цирконием. Большое внимание уделено корреляции характеристик взаимодействия в системе M–H с положением M в периодической системе элементов и оценке реализации этих корреляций применительно к системе Zr–H. Приведены сведения о диффузионной подвижности водорода в цирконии. Собираемые сведения ориентированы на создание исходной базы данных о взаимодействии в системе Zr–H, необходимой при проведении исследований по замедленному гидридному растрескиванию.

ВОДЕНЬ У ЦИРКОНІЇ
Частина 1

Т.П. Черняєва, А.В. Остапов

Систематизовані відомості про поведінку водню в цирконії. Пропоновані матеріали стосуються низки основних фізико-хімічних характеристик двох учасників реакції взаємодії Zr–H (H і Zr), а такоэ фундаментальних даних про систему Zr–H в цілому. Наводяться відомості про становище атомів водню в решітці Zr (переважно тетрагональні порожнечі) і цього динаміці. Слід зазначити, що дискусійним є питання щодо того, чи має розчинений у цирконії водень стан нейтральних атомів H^0 або іонів (H^+, H^-, $H^{\delta-}$, $H^{\delta+}$), в той же час однозначно стверджується, що водень в цирконії не зустрічається в молекулярному стані і не утворює пор, заповнених молекулярним газоподібним воднем. Викладено основні принципи взаємодії водню з металами (M). Представлена термодинаміка адсорбції і абсорбції водню цирконієм. Велику увагу приділено кореляції характеристик взаємодії в системі M–H з положенням M в періодичній системі елементів та оцінці реалізації цих кореляцій стосовно до системи Zr–H. Наведено відомості про дифузійну рухливість водню в цирконії. Зібрані відомості орієнтовані на створення вихідної бази даних про взаємодію в системі Zr–H, необхідної при проведенні досліджень по сповільненому гідридному розтріскуванню.